Static dielectric behavior of dipolar glasses

J. M. B. Lopes dos Santos
CFP, Departamento de Física, Faculdade de Ciências da Universidade do Porto, Rua do Campo Alegre 687, 4169-007 Porto, Portugal

M. L. Santos, M. R. Chaves, and A. Almeida
IMAT–Núcleo IFIMUP, Departamento de Física, Faculdade de Ciências da Universidade do Porto, Rua do Campo Alegre 687, 4169-007 Porto, Portugal

A. Klöpperpieper
Fachbereich Physik, Universität des Saarlandes, 66041 Saarbrücken, Germany
(Received 17 November 1999)

The understanding of the behavior of dipolar glasses has drawn heavily from the theory of conventional spin glasses. Nevertheless, some important aspects of the physics of dipolar glasses are absent in the spin systems. Because dipoles couple to electric rather than magnetic fields, quenched random fields, arising from lattice distortions, are almost always present in dipolar glasses. Also, in mixed families of compounds, like $(BP)_{1-x}(BPI)_x$ studied here, the end members of the series display clear quasi-one-dimensional character. We present here a systematic study of the static dielectric behavior in the paraelectric phase of this family of compounds and compare it to the predictions of several theoretical models. We were able to distinguish between quasi-one-dimensional and isotropic compounds, and to determine the values of parameters characterizing the interactions and the random electric fields; these, in turn, allow a determination of the Almeida-Thouless temperatures for the compounds with a glass phase. This work, together with structural and x-ray studies, leads to a detailed proposal for the phase diagram of this family of compounds.

I. INTRODUCTION

The study of low-temperature disordered phases in orientational glasses, and, particularly in dipolar glasses has drawn heavily from the theoretical development that has taken place in the past two decades in the field of spin glasses.[1] Both dipolar and spin glasses are characterized by competing interactions and disordered low-temperature phases. Nevertheless an important additional feature has to be considered when dealing with dipolar glasses. Substitutional disorder leads to lattice distortions that inevitably give rise to local quenched random electric fields, in addition to the usual random bond interactions. Lattice distortions cannot give rise to random magnetic fields unless time-reversal symmetry is broken. The existence of these random fields introduces some modifications of the properties of dipolar glasses relative to conventional magnetic spin glasses.[2]

Low temperature dipolar glass states have been reported to occur in solid solutions of betaine phosphate (BP) and betaine phosphite (BPI), $(BP)_{1-x}(BPI)_x$.[3–8] The basic structure of the BP and BPI compounds consists of quasilinear chains oriented parallel to the polar axis *b*; along the chains the PO_4 (BP) and PO_3 (BPI) groups are linked by hydrogen bonds.[9,10] The interaction between hydrogen bonds in adjacent chains is antiferroelectric for BP, and ferroelectric for BPI, while, within each chain, neighboring dipoles interact ferroelectrically both for BP and BPI.[11,12] The quasi-one-dimensional character of BP and BPI, already established in other works,[11,12] raises the possibility of considering the mixed $(BP)_{1-x}(BPI)_x$ compounds, which present experimental evidence of low temperature glass phases, as quasi-one-dimensional dipolar glasses. A model for this situation has been proposed by Orešič and Pirc.[13] However, a recent study of three compounds of this family failed to find significant differences between the predictions of quasi-one-dimensional models and isotropic models.[8] This may be due to the fact that these authors obtain the dielectric susceptibility from the Edwards-Anderson order parameter, using a result that is not valid for low-dimensional models.

In this paper, we report a systematic study of quasistatic dielectric behavior of the family of compounds $(BP)_{1-x}(BPI)_x$, in which we characterize the various low-temperature phases, determine the relevant interaction parameters and assess the dimensionality character of each compound. We compared our experimental data, in the paralelectric phase, with the predictions of three universal models: the quasi-one-dimensional Ising model without disorder[14,15] (I_{1D}) the isotropic Sherrington-Kirkpatrick model (SK),[16] with random fields, and the quasi-one-dimensional dipolar glass model of Orešič and Pirc (OP).[13] The Almeida-Thouless temperature,[17] which determines the limit of stability of the replica symmetric phase, and is usually taken to signal the onset of nonergodicity, was also estimated for the compounds with a glass phase. It should be stressed that, in the presence of random fields, the Edwards-Anderson order parameter, $q(T)$, is nonzero even in the high-temperature phase, and cannot be used to signal the onset of the glass phase.[2]

Using these results, in conjunction with other results reported in literature, we propose a detailed phase diagram for this family of compounds.

II. EXPERIMENTAL PROCEDURE

All the samples used in this work were cut as thin slices from high quality single crystals, grown form aqueous solu-

 ©2000 The American Physical Society

TABLE I. Summary of the measurement conditions of the complex dielectric constant for the family of compounds studied in this work.

x_{sol}	Rate (K/min)	$E_{a.c}$ (V/cm)	freq. (KHz)
0	1	10	10
0.15	1	10	1
0.40	1	10	10
0.50–0.97	0.3	1	1

tion by controlled solvent evaporation. Gold electrodes were evaporated on the faces perpendicular to the polar *b* direction. We denote by x_{sol} and x_{cr} the BPI content in the solution and the crystal, respectively. The latter, x_{cr} was determined from an x-ray analysis and also through a measurement of the single crystal density, as published elsewhere.[18] To allow comparison to other results in the literature we will normally use the nominal concentration x_{sol} to identify the compounds. However, the phase diagram will be presented in terms of the crystal concentration x_{cr}. The first colunm of Table II includes both these values, x_{cr} and x_{sol}.

Measurements of the complex dielectric constant as a function of temperature, at zero bias, were carried out with an Ando AG-4311 LCR meter, in slow heating, from 10 to 300 K. The measuring conditions are summarized in Table I. A closed cycle helium cryostat was used in the measurements.

III. THEORETICAL MODELS

We compared the inverse dielectric permittivity data, $1/\epsilon'(T)$, with the predictions of three models: the quasi-one-dimensional Ising model (I_{1D}),[14,15] the Sherrington-Kirkpatrick model with random fields, (SK) (Ref. 16) and the Orešič and Pirc model (OP).[13]

These models are all based on the following Ising Hamiltonian.

$$\mathcal{H}=-\frac{1}{2}\sum_{i,j} K_{ij}\sigma_i\sigma_j-\frac{1}{2}\sum_{i,j} J_{ij}\sigma_i\sigma_j-\sum_i h_i\sigma_i-F\sum_i \sigma_i. \tag{1}$$

The variables $\sigma_i=\pm 1$ denote the pseudo-spins. The first term represents the ordered part of the dipolar interaction, assumed of short range, and translationally invariant, i.e., $K_{ij}=K(\mathbf{R}_i-\mathbf{R}_j)$. The couplings J_{ij} are quenched random bonds, uncorrelated, drawn from a Gaussian distribution, identical for all pairs (ij)

$$P(J_{ij})=\frac{1}{\sqrt{2\pi J}}e^{-(J_{ij}-\overline{J}_0)^2/2\overline{J^2}}. \tag{2}$$

In order to have a thermodynamic limit the parameters $\overline{J}$ and $\overline{J}_0$ have to scale as

$$\overline{J}_0=\frac{J_0}{N};\quad \overline{J^2}=\frac{J^2}{N}. \tag{3}$$

The third term in Eq. (1) represents a random field also with a Gaussian distribution

$$P(h_i)=\frac{1}{\sqrt{2\pi}\Delta h}e^{-h_i^2/2\Delta h^2}. \tag{4}$$

The fourth term is the coupling to the external field *F*. Here, and in the following, we measure the external field in energy units (multiplied by μ, the dipole moment).

The I_{1D} (Refs. 14 and 15) model reflects the quasi-one-dimensional nature of the BP and BPI compounds by assuming that the dipoles are arranged along weakly coupled chains. The interaction between nearest neighbors along a chain *K*, is ferroelectric and in principle larger than the coupling between dipoles in different chains, which may be ferro or antiferroelectric. Disorder is not considered in this model, the random bonds J_{ij} and random fields h_i are taken to be zero. The interchain coupling is treated in mean field theory and can be characterized, in the paralectric phase, by a single parameter $K_\perp$.

The SK model takes the interactions to be purely random $(K_{ij}=0)$. The model is isotropic. The random bonds and fields are described by Eqs. (2) and (4). The Hamiltonian is characterized by the parameters, J_0, *J*, and Δh.

The OP model assumes a quasi one-dimensional structure as in the I_{1D} model. There is a nearest neighbor coupling between spins in the same chain, *K*, ferroelectric, but in addition, there is a random interaction given by Eq. (2) with zero mean $J_0=0$. The Hamiltonian is therefore characterized by *K*, *J*, and Δh.

In the following we review the main results of these models. We emphasize the prediction for the Edwards-Anderson order parameter $q(T)$ and the dielectric susceptibility.

Quasi-one-dimensional Ising model

The quasi-one-dimensional Ising model has been studied by several authors[14,15] and considers one dimensional chains of dipoles with intra-chain ferroelectric couplings, stronger than inter-chain ones. The coupling between chains is treated in mean-field theory. To consider the possibility of antiferroelectric ordering, transverse to the chains, one divides these into two sublattices. Denoting the two sublattice polarizations by $m_a=\langle\sigma_a\rangle$ and $m_b=\langle\sigma_b\rangle$ the corresponding equations are[15]

$$m_a=\frac{\exp(\beta K)\sinh(\beta F_a^{ef})}{[\exp(-2\beta K)+\exp(2\beta K)\sinh^2(\beta F_a^{ef})]^{1/2}} \tag{5}$$

$$m_b=\frac{\exp(\beta K)\sinh(\beta F_b^{ef})}{[\exp(-2\beta K)+\exp(2\beta K)\sinh^2(\beta F_b^{ef})]^{1/2}}a, \tag{6}$$

where the effective fields in each sublattice are given by

$$F_a^{ef} = F + 2K_\perp^{(1)} m_a + K_\perp^{(2)} m_b \tag{7}$$

$$F_b^{ef} = F + 2K_\perp^{(1)} m_b + K_\perp^{(2)} m_a, \tag{8}$$

where F is the external field and $K_\perp^{(1)}$ and $K_\perp^{(2)}$ characterize the couplings between chains of the same sublattice and different sublattices, respectively. In the paraelectric phase both polarizations go to zero as the external field vanishes and these equations may be expanded to linear order in the external field. One obtains for the susceptibility

$$\chi(T) \equiv n\mu^2 \frac{d(m_a + m_b)/2}{dF} = \frac{C/T}{\exp(-2\beta K) - \beta K_\perp}, \tag{9}$$

where $K_\perp = 2K_\perp^{(1)} + K_\perp^{(2)}$ and $C = n\mu^2/k_B$ is the Curie constant. The low temperature phase may be ferroelectric ($K_\perp^{(2)} > 0$) or antiferroelectric ($K_\perp^{(2)} < 0$). In either case, Eq. (9) holds for the susceptibility, down to the transition temperature given by the solutions of

$$\beta_c (2K_\perp^{(1)} + K_\perp^{(2)}) = \exp(-2\beta_c K) \tag{10}$$

in the ferrolectric case and

$$\beta_N (2K_\perp^{(1)} - K_\perp^{(2)}) = \exp(-2\beta_N K) \tag{11}$$

in the antiferroelectric one. Note that in the ferrolectric case T_c can be estimated from a fit to $\chi(T)$ in the paralectric phase, whereas in the antiferroelectric case we obtain only a lower bound for T_N by assumming $K_\perp^{(1)} = 0$ ($K_\perp^{(2)} = K_\perp$).

Sherrington-Kirkpatrick model

The extension of the Sherrington-Kirkpatrick model to include random fields can be found in Ref. 2. Applying the replica trick and the steepest descent method one arrives at the following equations for the polarization $m(T) \equiv \langle\langle \sigma_i \rangle\rangle_J$ per site and for the Edwards-Anderson order parameter $q(T) \equiv \langle\langle \sigma_i \rangle^2\rangle_J$:

$$m(T) = \frac{1}{\sqrt{2\pi}} \int_{-\infty}^{+\infty} ds e^{-s^2/2} \tanh[\beta \eta(s)] \tag{12}$$

$$q(T) = \frac{1}{\sqrt{2\pi}} \int_{-\infty}^{+\infty} ds e^{-s^2/2} \tanh^2[\beta \eta(s)], \tag{13}$$

where $\eta(s)$ is an effective mean field given by

$$\eta(s) = J_0 m + \sqrt{J^2 q + \Delta h^2}\, s + F. \tag{14}$$

The thermal average (Boltzmann weight) is denoted by $\langle \ldots \rangle$. The quenched average over the distribution of random fields and bonds is denoted by $\langle \ldots \rangle_J$. These equations have to be solved self-consistently for m and q. They simplify considerably for non-polar phases, $m = 0$. By deriving the Eq. (12) with respect to the external field one obtains for the zero field susceptibility in a nonpolar phase[16]

$$\chi(T) = \frac{n\mu^2}{k_B} \frac{1 - q(T)}{T - (J_0/k_B)[1 - q(T)]}$$

$$= C \frac{1 - q(T)}{T - (J_0/k_B)[1 - q(T)]}. \tag{15}$$

The expression of Eq. (15) was fitted to the experimental data by varying the parameters C, the Curie constant, J_0, J, and Δh. An iterative, nonlinear least-squares fitting procedure was used. In each iteration Eqs. (12), (13), and (14) are solved to determine the value of $q(T)$. The onset of a ferroelectric phase is signaled by a divergence of $\chi(T)$. The Curie temperature is therefore determined by [see Eq. (15)]

$$q(T_c) = 1 - \frac{k_B T_c}{J_0}. \tag{16}$$

Since $q(T)$ is independent of J_0 for a nonpolar phase, we could easily check, given $q(T)$, that in none of the compounds to which we were able to fit this model, was J_0 large enough to give rise to a ferroelectric instability.

It is quite clear from Eqs. (13) and (14), that in the presence of random fields the high temperature phase will have a nonzero value of $q(T)$. As a result the onset of a glass phase is not determined by the appearance of a nonzero value of $q(T)$. However, it is well known[1,17] that the replica symmetric solution we have presented becomes unstable below the Almeida-Thouless temperature. This instability also occurs in the presence of random fields and is usually associated with the onset of nonergodicity. The Almeida-Thouless temperature T_{AT} is given by[2]

$$\left(\frac{k_B T_{AT}}{J}\right)^2 = \int_{-\infty}^{\infty} \frac{ds}{\sqrt{2\pi}} e^{-s^2/2} [1 - \tanh^2(\beta \eta(s)]^2 \tag{17}$$

and can be determined once J and Δh are obtained from the fits to the dielectric susceptibility.

Orešič and Pirc model

The Orešič and Pirc (OP) model is an anisotropic version of the SK model. The dipoles are assumed to be arranged in one dimensional chains, with a ferroelectric coupling K between nearest neighbors in each chain. An SK type long-range random bond interaction, with zero mean, $J_0 = 0$, exists between all pairs of spins (within a chain and between chains). Using the replica trick and averaging over the random bond and random field distributions, one obtains a free energy per dipole given by

$$\mathcal{F} = -\frac{J^2}{4k_B T}(1 - q^2) + \langle \mathcal{F}_{1D} \rangle_{s_i}, \tag{18}$$

where $\mathcal{F}_{1D} = -(\beta N)^{-1} \log \mathrm{Tr} \exp(-\beta \mathcal{H}_{1D})$ is the free energy corresponding to a one dimensional Ising model in a random field,

$$\mathcal{H}_{1D} = -\sum_i K \sigma_i \sigma_{i+1} - \sum_i \eta(s_i) \sigma_i, \tag{19}$$

with $\eta(s)$ still given by Eq. (14), with $J_0 = 0$. The symbol $\langle \ldots \rangle_{s_i}$ denotes an average over N independent random variables with a Gaussian distribution of zero mean and unit root mean square deviation,

$$P(s_i) = \frac{1}{\sqrt{2\pi}} e^{-s_i^2/2}. \tag{20}$$

Whereas in the SK model one ends up with an effective single spin problem in a random effective field the OP model gets reduced to an interacting one-dimensional Ising model in a random effective field. There is no known closed form solution for this model. Orešič and Pirc used a numerical recursion method introduced by Fan and McCoy[19] and Andelman.[20]

The method requires consideration of a finite chain of N dipoles. A realization of the random variables s_i, $i=1,\ldots,N$ is made. Denoting by $x_i \equiv \exp[-2\beta\eta(s_i)]$, $v \equiv \exp(-2\beta K)$ the local polarization can be shown to be given by[13]

$$\langle\sigma_i\rangle_{1D}=\frac{x_i-z_iy_i}{x_i+z_iy_i}, \tag{21}$$

where the quantities z_i and y_i are determined by the following recursion relations and boundary conditions

$$z_i=vx_i\frac{1+z_{i-1}/v}{1+z_{i-1}v}; \quad z_1=x_1 \tag{22}$$

$$y_i=vx_i\frac{1+y_{i+1}/v}{1+y_{i+1}v}; \quad y_N=x_N. \tag{23}$$

The values of m and q are given by the equations

$$m(T)=\frac{1}{N}\sum_i \langle\sigma_i\rangle_{1D} \tag{24}$$

$$q(T)=\frac{1}{N}\sum_i \langle\sigma_i\rangle_{1D}^2. \tag{25}$$

Naturally, for finite N these quantities will show statistical fluctuations. To obtain the susceptibility Orešič and Pirc calculate $m(T,F)$ for a small external field F and use $\chi=n\mu^2 m(T,F)/F$. As $m(T,F)$ goes to zero as $F\to 0$, statistical fluctuations become severe and the method requires very large samples. We followed a slightly different method. By expanding the recursion relations for z_i and y_i and Eq. (21) to linear order in the external field, and defining $\langle\sigma_i\rangle_{1D}=\langle\sigma_i\rangle_{1D}^0+\chi_i F$, we obtained the following expression for χ_i (see Appendix),

$$\chi_i=-\langle\sigma_i\rangle_{1D}^0\left(\frac{\gamma_iy_i+\rho_iz_i+2\beta x_i}{x_i-z_iy_i}+\frac{\gamma_iy_i+\rho_iz_i-2\beta x_i}{x_i+z_iy_i}\right), \tag{26}$$

where γ_i and ρ_i are determined by the following recursion relations

$$\gamma_i=-2\beta z_i+z_i\gamma_{i-1}\left(\frac{1/v}{1+z_{i-1}/v}-\frac{v}{1+vz_{i-1}}\right) \tag{27}$$

$$\gamma_1=-2\beta z_1 \tag{28}$$

$$\rho_i=-2\beta y_i+y_i\rho_{i+1}\left(\frac{1/v}{1+y_{i+1}/v}-\frac{v}{1+vy_{i+1}}\right) \tag{29}$$

$$\rho_1=-2\beta y_N. \tag{30}$$

The susceptibility is given by

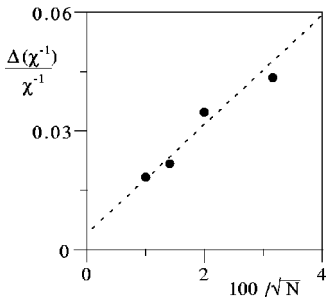

FIG. 1. Statistical fluctuations of the calculated inverse susceptibility, $\Delta\chi/\chi^{-1}$, in the OP model, as function of $1/\sqrt{N}$ where N is the number of dipoles used in the recursion method.

$$\chi(T)=Ck_B\frac{1}{N}\sum_i \chi_i. \tag{31}$$

To calculate the susceptibility one starts by generating N random numbers drawn from the distribution of Eq. (20). Using an initial guess of the fitting parameters, C, K, J, and Δh, the Eqs. (21) to (25) have to be solved self-consistently for $q(T)$ and $m(T)$ which enter the right hand side of these equations through the parameter $\eta(s)$ [Eq. (14)]. The susceptibility can then be calculated using Eqs. (27) to (30) and Eq. (31). Its value is compared to the experimental susceptibility and a nonlinear least squares fitting routine determines new values of C, K, J, and Δh. The process is iterated until it converges to a best fit (in least squares sense). The initial N random numbers are not changed in this process.

To assess the importance of statistical fluctuations, we repeated ten times the calculation of $\chi(T)$ at a particular (low) temperature, for various lattice sizes. We found that $\Delta\chi^{-1}/\chi^{-1}\approx 1.5/\sqrt{N}$ (see Fig. 1). For our final fits we used lattices with $N=10000$, statistical fluctuations being below 2%.

We would like to point out that Eq. (15) is not valid for the OP model. This relation was used in Ref. 8, along with the equations of the OP model for the order parameter $q(T)$. It can be shown that, in this model, the following equation holds,[13]

$$\chi(T)=\frac{C}{T}\left(1-q(T)+\frac{2}{N}\sum_{(ij)}\langle\sigma_i\sigma_j\rangle_{1D}\right) \tag{32}$$

and so, using Eq. (15), introduces a new parameter that is not in the model, and neglects one-dimensional correlations, in clear contradiction with the aims of the OP model.

Replica symmetry breaking also occurs in this model. We estimated the Almeida-Thouless temperatures, for each compound fitted by this model, using the data published in the Orešič and Pirc paper.[13]

IV. RESULTS AND DISCUSSION

The dielectric constant $\epsilon'(T)$ can be written as

$$\epsilon'(T)=\epsilon_\infty+\chi(T) \tag{33}$$

were the first term includes the nondipolar contributions. In our analysis, we assumed that $\chi(T)\gg\epsilon_\infty$, i.e., $1/\chi(T)\approx 1/\epsilon'(T)$. As a check we analyzed some of the compounds using only data with $\epsilon(T)>100$ without significant changes

TABLE II. Values of interaction parameters obtained from the best fits to the models I_1D, SK, and OP, for the compounds of the family $(BP)_{1-x}(BPI)_x$ for the chosen concentrations. x_{sol} is the concentration in the crystal growing solution and $x_{cr}$the crystal concentration as determined by x-ray diffraction (Ref. 18). All interaction parameters are given in Kelvin. The temperatures T_{AT} for the OP fits were estimated from the results of Ref. 13.

x_{cr}/x_{sol}	Best fit(s)	T_c	T_{AT}	K	J_0	$K_\perp$	J	Δh	C
0/0	I_{1D}	85		91		−10			11755
0.08/0.15	OP		82	78			64	14	11736
0.25/0.40	SK		48		71		86	42	14480
0.33/0.50	SK		52		55		83	30	9030
0.54/0.70	SK(OP)		26(22)	−(46)	41(−)		66(51)	65(72)	16494(13492)
0.67/0.80	SK(OP)		29(24)	−(52)	57(−)		72(50)	69(71)	17178(14602)
0.74/0.85	SK(OP)		43(57)	−(63)	94(−)		89(64)	62(36)	18958(17182)
0.82/0.90	SK		47		116		94	60	7347
0.89/0.94	I_{1D}	106		208		2			8382
0.94/0.97	I_{1D}	177		279		8			6290

in the results. We studied data for 10 compounds of the family $(BP)_{1-x}(BPI)_x$, spanning the entire range of concentrations. As a starting criterium for the limit of the paraelectric phase we used the minimum of $1/\epsilon'(T)$, and fitted the data above that temperature up to room temperature to the predictions of the three models mentioned above.

One salient feature of the data for all the compounds is the pronounced curvature of the plots of $1/\epsilon'(T)$ against T. Curie-Weiss behavior is not observed up to room temperature. There are two possible sources for this curvature. The susceptibility of a one dimensional chain [Eq. (9), with $K_\perp = 0$] is the high-temperature limit of both the I_{1D} and the OP models and shows pronounced curvature even for $k_BT > K$. Curie-Weiss fits in narrow temperature ranges can grossly overestimate the Curie constant, C. On the other hand, it follows from Eq. (15), that the SK model predicts strict Curie-Weiss behavior, in the absence of random fields, in the paraelectric phase ($q=0$). However, in the presence of random fields $q(T)$ is nonzero at all temperatures and the growth of $q(T)$, as the temperature lowers, gives rise to an upward curvature of $1/\chi$ vs T.

Our analysis allows a detailed assessment of the relative importance of these two effects (quasi-one-dimensionality and random fields) in the various compounds. We will now discuss them in turn. The parameters obtained from the fits, as well as the corresponding transition or Almeida-Thouless temperatures are shown in Table II.

Concentrations $x_{sol}=0$, 0.94, and 0.97

These compounds are rather well fitted by the I_{1D} model, as shown in Fig. (2) for the $x_{sol}=0.97$ compound. For the $x_{sol}=0.94$ and 0.97 compounds the data deviates slightly from the fit close to T_c but a satisfactory fit to either of the disorder models could not be made. The parameters obtained confirmed the antiferroelectric nature of BP and the ferroelectric nature of the compounds with $x_{sol}=0.94$ and 0.97. Note that, as expected, the interchain couplings turn out to be much smaller than the intrachain ones (see Table II).

Compound with $x_{sol}=0.15$

In Fig. 3 we compare the experimental data on this compound to the the predictions of the models we are considering. It is quite clear that the SK model does not fit the data, and that I_{1D} predictions deviate substantially from the data in a 30 K vicinity of the maximum of $\epsilon'(T)$; also, this model predicts an antiferroelectric transition above 106 K. In fact, we find a similar situation in the remaining compounds: fits to the I_{1D} model give predictions for antiferroelectric transition temperatures well above the maxima of the dielectric constant, where in fact no sign of a transition is present. Therefore, we shall not discuss this model any further. The OP model fits the data for $(BP)_{0.85}(BPI)_{0.15}$ quite well in the entire temperature region considered. The parameters determined by the fit, shown in Table II, predict an Almeida-Thouless temperature of 82 K almost coincident with the lower temperature considered in the fit. Another aspect to consider is whether the parameters we found for the intrachain interaction K and the interchain one J are consistent with the assumption of weakly coupled chains. The correct way to compare these two interactions, is, however, disputable, since K is a nearest neighbor interaction and J an infinite range one. One way to proceed is to compare the interactions of one dipole with all its neighbors, i.e., $2K$ and J, and we find $(2K) \approx 2.5J$, i.e., a moderately larger intrachain coupling. This compound shows the first convincing evidence of a quasi-one-dimensional glass phase predicted by the OP model.

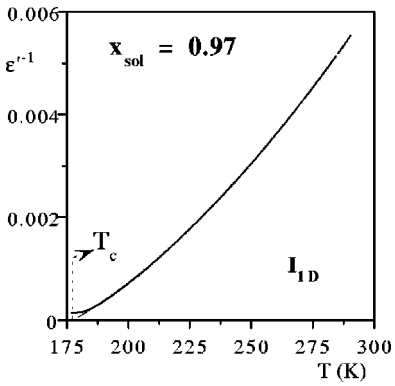

FIG. 2. The inverse real dielectric constant $1/\epsilon'(T)$ of the $(BP)_{0.03}(BPI)_{0.97}$ compound fitted to the I_{1D} prediction. The thicker line is the data, the thinner one the fit.

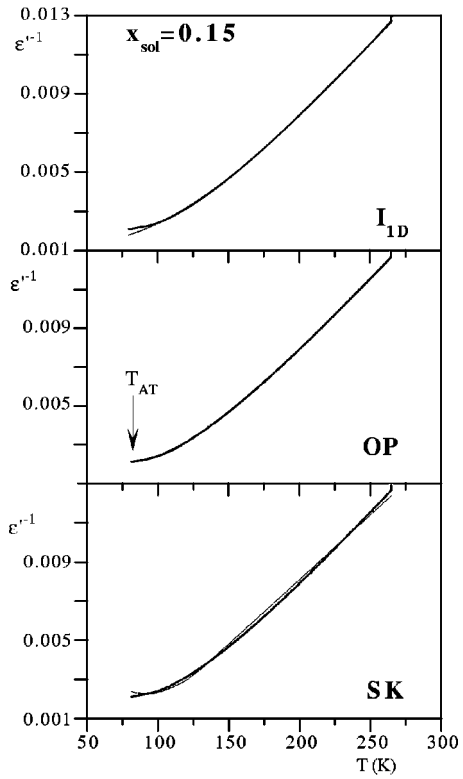

FIG. 3. The inverse real dielectric constant $1/\epsilon'(T)$ of the $(BP)_{0.85}(BPI)_{0.15}$ compound fitted to I_{1D}, OP and SK predictions. The thicker lines are the data, the thinner ones the fits.

Concentrations $x_{sol}=0.40$ and 0.50

Somewhat surprisingly, we found that these compounds are unambiguously better fitted by the SK model (see Fig. 4 for the $x=0.40$ compound). The OP fits are clearly off the mark at low temperatures and give values of $(2K)\approx J$, i.e., same order of magnitude for intra and interchain coupling, undermining the assumption of weakly coupled chains. There is no evidence of quasi-one-dimensionality in these compounds. The random field parameter Δh is at least double from the $x_{sol}=0.15$ compound, reflecting the increased disorder, which is probably related to the loss of the quasi-one-dimensional character. It is also curious that the random bond interactions display a marked ferroelectric character ($J_0\approx J$) despite the fact that these compounds have only a small BPI content ($x_{cr}=0.25$ and 0.33).

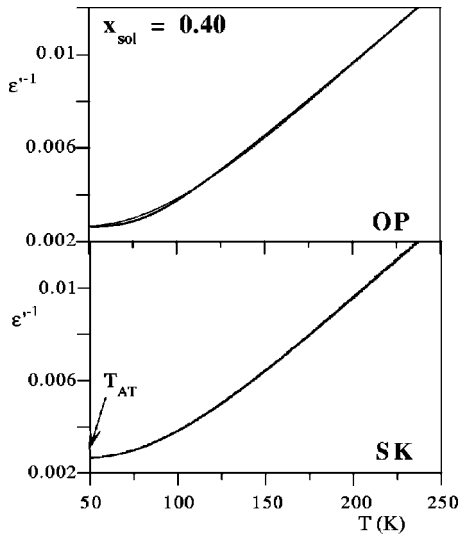

FIG. 4. The inverse real dielectric constant $1/\epsilon'(T)$ of the $(BP)_{0.60}(BPI)_{0.40}$ compound fitted to the SK model. The fit to the OP model is clearly less satisfactory. Similar results are found for the $(BP)_{0.50}(BPI)_{0.50}$ compound.

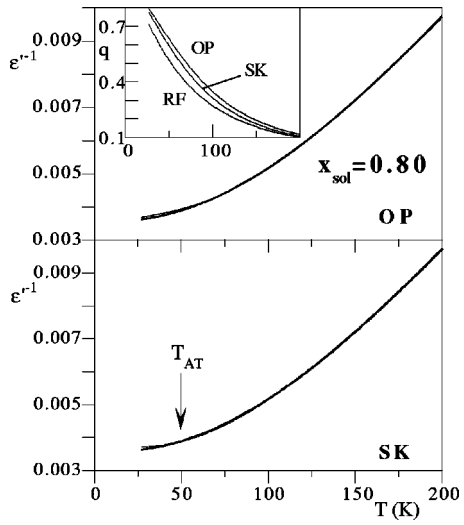

FIG. 5. The inverse real dielectric constant $1/\epsilon'(T)$ of the $(BP)_{0.20}(BPI)_{0.80}$ can be fitted just as well to the SK model and OP models. The inset shows the values of the Edwards-Anderson order parameter, calculated with these two models and also including only random fields, with the same Δh as in the fits.

Concentrations $x_{sol}=0.70$ and 0.80

In this range of concentration, data can be fitted almost equally well by the SK and OP models (see Fig. 5 for the $x_{sol}=0.80$). In our opinion, this is due to the fact that the random fields are a dominant effect in these compounds. In the inset of Fig. 5 we illustrate this by showing the values of the order parameter, $q(T)$, given by both models and also by assuming that all the interactions, with the exception of the random field term are zero (we used the value of $\Delta h=70$, the values obtained from the fits being $\Delta h/k_B=69$ K, SK, and 71 K, OP). For these values of fields, and in this temperature range, the interactions give relatively small corrections to the random fields and the predictions of the two models become very similar.

Concentrations $x_{sol}=0.85$ and 0.90

In the first of these compounds the SK and OP fits are of similar quality. However, unlike in the previous group the estimates of the random field parameter are quite different, the OP model giving much smaller values (see Table II). In the $x_{sol}=0.90$ compound a similar thing happens but in this case the fit to the OP model is very poor (Fig. 6).

A consistent picture seems to emerge from these results. Even though the end members of the series show quasi-one-dimensional character, in the compounds with a glass phase the OP model is clearly adequate only for the $x_{sol}=0.15$ compound which has relatively small random fields ($\Delta h/k_B=14$ K). As soon as the random fields become comparable to other interaction parameters (see Fig. 7) the SK, isotropic model, gives a better (or at least as good) representation of

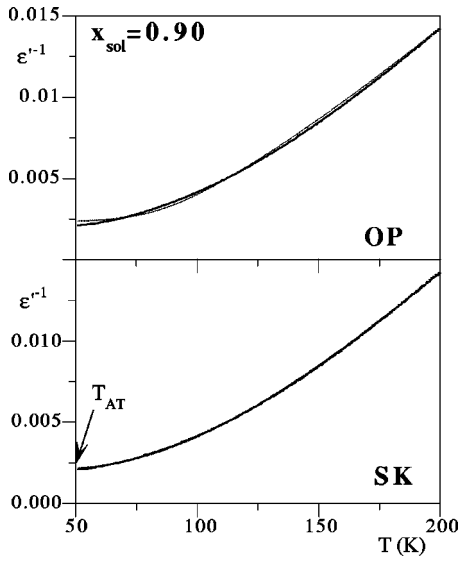

FIG. 6. The inverse real dielectric constant $1/\epsilon'(T)$ of the $(BP)_{0.10}(BPI)_{0.90}$ fitted to the OP and SK models.

the data. Since the random fields reflect lattice disorder, it is not unreasonable, that in a strongly disordered lattice the quasi-one-dimensional character should be destroyed. One immediate consequence of the existence of significant random fields, is that the Edwards-Anderson order parameter, $q(T)$ has nonzero values in whole temperature range, as can be seen in Fig. 8. At high temperatures this is a single dipole effect and would be present even without dipolar interactions. Within the context of these models, one cannot distinguish the system's phase, at these temperatures, from what happens at infinite temperatures where the dipoles are completely free. The freezing of the dipoles, displayed in the nonzero values of $q(T)$, and in the deviation of the inverse dielectric susceptibility from Curie-Weiss behavior, should not be used to identify the onset of a glass phase when random fields are present. However, the OP and SK models allow the determination of the Almeida-Thouless temperature below which their corresponding solutions are no longer stable due to replica symmetry breaking.[17,13] From the parameters of the fits we were able to estimate these temperatures, shown in Fig. 7.

The compounds with larger values of random fields display, not only the larger values of $q(T)$, but also the lower values of T_{AT}. The breaking of the replica symmetry is usually associated with the onset of nonergodicity, which results

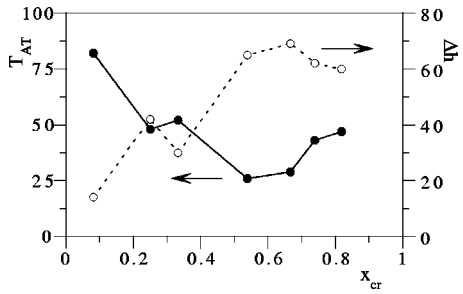

FIG. 7. The root mean square deviation, Δh of the local random fields, and the Almeida-Thouless temperatures as a function of the BPI content x_{cr}, in the crystal.

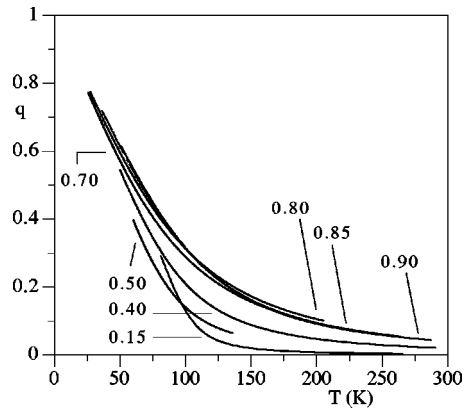

FIG. 8. The Edwards-Anderson order parameter $q(T)$ for various compounds. Its values are significantly nonzero well above the Almeida-Thouless temperatures.

from the many valley structure of the free energy in phase space. As stated above, if random fields dominate, the ground state of the system is uniquely defined, each dipole pointing in the direction of the field at its site. So it is not surprising that the highest values of Δh should be associated with the lowest values of T_{AT}. The lowest T_{AT} occurs for the compound that has a BPI concentration in the crystal $x_{cr} = 0.54$ (see Fig. 7).

In Fig. 9 we depict the variation of the interaction parameters with the concentration of BPI, x_{cr}. Variations of the parameters of the SK model are within a factor of two (even less for the case of J) but the intrachain coupling, K, is clearly much stronger for the compounds with BPI concentration approaching unity.

The phase diagram

This study, in conjunction with other results reported in the literature suggests a detailed phase diagram of the family of compounds $(BP)_{1-x}(BPI)_x$; we depict it in Fig. 10 as a function of BPI content in the crystal (x_{cr}). We include both the dielectric and structural characterization of the different phases, and indicate the concentration ranges where the quasi-one-dimensional character is present and those where it is not manifest.

All the compounds have a high-temperature ferrodistortive paralectric phase (PE) with $P12_1/c1$ symmetry.[18,21] Our fit to the I_{1D} confirms the antiferroelectric nature of BP. The

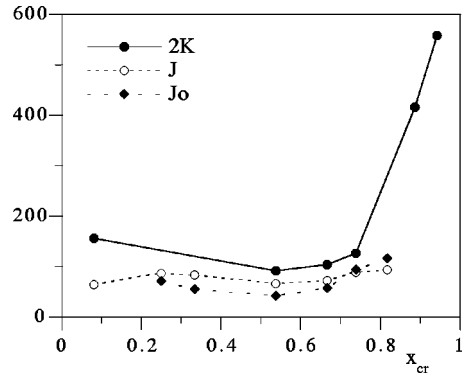

FIG. 9. The interaction parameters as a function of BPI content in the crystal.

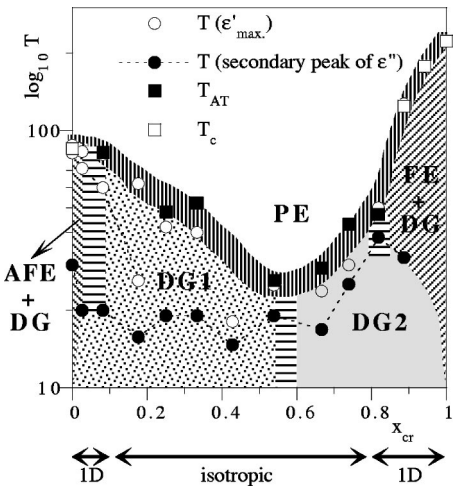

FIG. 10. A proposed phase diagram for the compounds $(BP)_{1-x}(BPI)_x$, shown here in terms of the BPI content of the crystal x_{cr}.

parameters we obtained are similar to those reported by Fisher *et al.*[11] Below 81 K pure BP has an antiferroelectric phase, with 8 BP molecules per unit cell, and the same symmetry group as the paraelectric phase, $P12_1/c1$.[22] The work of several groups has established the existence of an intermediate phase between 86 K and 81 K,[21,22] with 4 BP molecules per unit cell.[22] It was found to be a polar phase, with symmetry group $P12_11$.[5,6,23] Given the fact that interchain couplings, as determined by the fits in the paraelectric phase, are antiferroelectric, this is, most likely, a ferrielectric phase. The I_{1D} fit predicts $T_c = 85$ K.

The pure BPI compound is ferroelectric[21] ($T_c = 222$ K) and the critical behavior is well described by a Landau theory, with exponents close to those of a tricritical transition.[23]

Compounds with small content of BPI show the same phase sequence, as pure BP.[5,6] The compounds with large BPI content studied here, $x_{cr} = 0.89$, 0.94, are still ferrolectric and quasi-one-dimensional. Nevertheless, all these compounds, near the end members of the series, display some evidence of disorder. Studies of the complex dielectric constant as a function of frequency and temperature,[5,23] show that the imaginary part of the dielectric permittivity, $\epsilon''(T)$, has a secondary broad peak, well below the temperature of the maximum of $\epsilon'(T)$, and which shifts to higher temperatures as the frequency increases. These maxima of $\epsilon''(T)$ are signalled by the filled circles in Fig. 10. Polarization measurements, through the pyroelectric effect, in the ferroelectric compounds, $x_{cr} = 0.89$ and 0.94, display very broad transition regions.[5] In this paper we found a rounding of the peak of the dielectric permittivity $\epsilon'(T)$ relative to the prediction of the I_{1D} model. We refer to these antiferro and ferroelectric phases with disorder, as AFE+DG and FE+DG respectively.

In the range of concentrations $0.08 \leqslant x_{cr} \leqslant 0.80$ static dielectric behavior is consistent with a low-temperature glass phase. The compounds with small BPI content show evidence of quasi-one-dimensionality. Measurements of complex dielectric constant, show symmetric profiles of $\epsilon''(\ln \omega)$ for compounds with larger BPI content ($x_{sol} = 0.80, 0.85$) (Refs. 8 and 24) and strongly asymmetric ones for smaller concentrations of BPI ($x_{sol} = 0.05, 0.15, 0.30, 0.38, 0.50, 0.60$).[3,4,8] We identified these types of glass phases as DG2 and DG1, respectively. We calculated the Almeida-Thouless temperatures, which we take to signal the onset of a nonergodic glass phase, for these compounds. The phase diagram also indicates other characteristic temperatures, like the temperature of the maxima of the low frequency real dielectric permittivity, $\epsilon'(T)$, and the temperature of the secondary broad peak in the low frequency imaginary part of the dielectric constant $\epsilon''(T)$, alluded to above. We should stress the temperatures of the maxima of $\epsilon'(T)$ track, reasonably well, the Almeida-Thouless temperatures, in the available range of concentrations.

In the phase diagram of Fig. 10 we indicate the diffuse nature of the transition from the paraelectric phase by tracing bold vertical dashes around the Almeida-Thouless temperature, throughout the phase diagram. The horizontal dashes are meant to suggest the uncertainty in the precise concentration limits for the different phases.

V. CONCLUSIONS

We presented a systematic study of the dielectric properties of compounds of the series $(BP)_{1-x}(BPI)_x$, in the paraelectric phase, and confronted them with the predictions of three microscopic models: the quasi-one-dimensional Ising model without disorder, the Sherrington-Kirkpatrick (SK) model and the Orešič and Pirc (OP) model. This analysis allowed a quantitative determination of the parameters characterizing the dipolar interactions and the random electric fields in this system.

In one of the compounds (concentration x, as determined by x-ray analysis, of 0.08) we found a behavior consistent with a quasi one-dimensional glass phase predicted by the OP model. However, there was no evidence of quasi-one-dimensional behavior for compounds with a higher concentration of BPI except for nearly pure, ferroelectric BPI. In fact, the other compounds with a glass phase are rather well fitted by the SK model with the inclusion of random fields. Although the symmetry group of these compounds is consistent with a chain like structure, substitutional disorder induces an isotropic dielectric behavior, i.e., interchain and intrachain couplings are of similar magnitude. The correlation between increasing randomness and loss of quasi-one-dimensional dielectric behavior is manifest in the fact that the root mean square deviation of the random field, Δh, when compared to other interaction parameters, is much smaller in the compound fitted to the OP model than in any of the compounds described by the SK model. The deviations from Curie-Weiss behavior, seen in these compounds up to room temperature, are due to the existence of significant random electric fields. The SK model, without random fields, predicts strict Curie-Weiss behavior down to the freezing temperature.

We were able to estimate the Almeida-Thouless temperatures for all the compounds with a glass phase. We found it to be close to the temperature at which the real part of the low frequency dielectric constant, has a maximum, throughout the entire family of compounds, thereby justifying the common practice of identifying the onset of the glass phase

with the maximum of $\epsilon'(T)$. On the other hand, the Almeida-Thouless temperatures are determined essentially by the magnitude of the random field (Fig. 7). A somewhat amusing result of this study, is that *the samples with greater lattice disorder, i.e., greater random fields, show the lowest temperatures for the onset of the glass phase*. Our interpretation of this apparently surprising result, is that the quenched random fields arising from lattice disorder, determine a well defined, preferred orientation for each dipole, thereby simplifying the many-valley structure of phase-space, and pushing a nonergodic glass phase to lower temperatures.

ACKNOWLEDGMENTS

We would like to acknowledge financial support from Praxis XXI, Projects Nos. 2/2.1/FIS/26/94 and 2/2.1/FIS/302/94.

APPENDIX: CALCULATION OF SUSCEPTIBILITY IN THE OREŠIČ PIRC MODEL

We start by defining the expansions of the quantities z_i, y_i, and $\langle\sigma_i\rangle_{1D}$, defined in the main text to linear order in the external field F:

$$z_i = z_i^0 + \gamma_i F + O(F^2) \tag{A1}$$

$$y_i = y_i^0 + \rho_i F + O(F^2) \tag{A2}$$

$$\langle\sigma_i\rangle_{1D} = \langle\sigma_i\rangle_{1D}^0 + \chi_i F + O(F^2) \tag{A3}$$

$$x_i = x_i^0(1-2\beta F) + O(F^2). \tag{A4}$$

Expanding the recursion relations for z_i and y_i [Eqs. (22) and (23)] and gathering the terms linear in F, one readily derives the following recursion relations for the γ's and $\rho's$

$$\gamma_i = z_i^0\left[-2\beta + \gamma_{i-1}\left(\frac{1/v}{1+z_{i-1}^0/v} - \frac{v}{1+vz_{i-1}^0}\right)\right] \tag{A5}$$

$$\rho_i = y_i^0\left[-2\beta + \rho_{i+1}\left(\frac{1/v}{1+y_{i+1}^0/v} - \frac{v}{1+vy_{i+1}^0}\right)\right]. \tag{A6}$$

The end conditions, $\gamma_1 = -2\beta z_1$ and $\rho_N = -2\beta y_N$ follow directly from the definitions $z_1 = x_1 = \exp[-2\beta\eta(s_1)]$, $y_N = x_N = \exp[-2\beta\eta(s_N)]$ and $\eta(s) = \sqrt{J^2q + \Delta h^2 s} + F$. Inserting these equations into the equation for $\langle\sigma_i\rangle_{1D}$ and gathering the linear terms one obtains

$$\chi_i = -\langle\sigma_i\rangle_{1D}^0\left(\frac{\gamma_i y_i^0 + \rho_i z_i^0 + 2\beta x_i}{x_i^0 - z_i^0 y_i^0} + \frac{\gamma_i y_i^0 + \rho_i z_i^0 - 2\beta x_i^0}{x_i^0 + z_i^0 y_i^0}\right). \tag{A7}$$

This equation and the two previous ones are precisely Eqs. (26), (27), and (29) with the zero superscripts dropped with the understanding that all quantities on the right hand side are calculated in zero field. Given a set of random values s_i, $i=1,\ldots N$, the recursion relations given by Eqs. (22) and (23),[13] and Eqs. (27) and (29) completely define the quantities z_i, y_i, γ_i, and ρ_i, which enter into the definition of χ_i [Eq. (26)].

[1] K. Binder and A.P. Young, Rev. Mod. Phys. **58**, 801 (1986); U.T. Höchli, K. Knorr, and A. Loidl, Adv. Phys. **39**, 405 (1990).

[2] R. Pirc, B. Tadić, and R. Blinc, Phys. Rev. B **36**, 8607 (1987).

[3] S.L. Hutton, I. Fehst, R. Böhmer, M. Braune, B. Mertz, P. Lunkenheimer, and A. Loidl, Phys. Rev. Lett. **66**, 1990 (1991).

[4] S.L. Hutton, I. Fehst, R. Böhmer, and A. Loidl, Ferroelectrics **127**, 279 (1992).

[5] M.L. Santos, J.C. Azevedo, A. Almeida, M.R. Chaves, A.R. Pires, H.E. Müser, and A. Klöpperpieper, Ferroelectrics **108**, 363 (1990); M.L. Santos, M.R. Chaves, A. Almeida, A. Klöpperpieper, H.E. Müser, and J. Albers, Ferroelectric Lett. **15**, 17 (1993).

[6] M. Lopes dos Santos, J.M. Kiat, A. Almeida, M.R. Chaves, A. Klöpperpieper, and J. Albers, Phys. Status Solidi B **189**, 371 (1995).

[7] J. Banys, C. Klimm, G. Völkel, H. Bauch, and A. Klöpperpieper, Phys. Rev. B **50**, R16 751 (1994); J. Banys, C. Klimm, G. Völkel, R. Böttcher, H. Bauch, and A. Klöpperpieper, J. Phys.: Condens. Matter **8**, L245 (1996).

[8] H. Ries, R. Böhmer, I. Fehst, and A. Loidl, Z. Phys. B: Condens. Matter **99**, 401 (1996).

[9] W. Shildkamp and J. Spilker, Z. Kristallogr. **168**, 159 (1984).

[10] I. Fehst, M. Paasch, S.L. Hutton, M. Braune, R. Böhmer, A. Loidl, M. Dörffel, T.H. Narz, S. Haussühl, and G.J. McIntyre, Ferroelectrics **138**, 1 (1993).

[11] G. Fisher, H.J. Brückner, A. Klöpperpieper, H.G. Unruh, and A. Levstik, Z. Phys. B: Condens. Matter **79**, 301 (1990).

[12] H. Bauch, R. Bötcher, and G. Völkel, Phys. Status Solidi B **178**, K39 (1993); **179**, K41 (1993).

[13] M. Orešič and R. Pirc, Phys. Rev. B **47**, 2655 (1993).

[14] A.V. de Carvalho and S.R. Salinas, J. Phys. Soc. Jpn. **44**, 238 (1978).

[15] R. Blinc, B. Žekš, A. Levstik, C. Filipič, J. Slak, M. Burgar, I. Zupančič, L.A. Shuvalov, and A.I. Baranov, Phys. Rev. Lett. **43**, 231 (1979); R. Blinc and F.C. Sa Barreto, J. Chem. Phys. **72**, 6031 (1980).

[16] David Sherrington and Scott Kirkpatrick, Phys. Rev. Lett. **35**, 1792 (1975).

[17] J.R.L. de Almeida and D.J. Thouless, J. Phys. A **11**, 983 (1978).

[18] M.L. Santos, L.C.R. Andrade, M.M.R. Costa, M.R. Chaves, A. Almeida, A. Klöpperpieper, and J. Albers, Phys. Status Solidi B **199**, 351 (1997).

[19] C. Fan and B.M. McCoy, Phys. Rev. **182**, 614 (1969).

[20] D. Andelman, Phys. Rev. B **34**, 6214 (1986).

[21] J. Albers, A. Klöpperpiper, H.J. Rother, and K.H. Ehses, Phys. Status Solidi A **74**, 553 (1982); J. Albers, A. Klöpperpiper, H.J. Rother, and S. Haussühl, Ferroelectrics **81**, 991 (1988).

[22] O. Freitag, H.G. Brückner, and H.G. Unruh, Z. Phys. B: Condens. Matter **61**, 75 (1985).

[23] M. L. Santos, Ph.D. thesis, University of Porto, 1999.

[24] J. M. B. Lopes dos Santos, M. L. Santos, M. R. Chaves, A. Almeida, and A Klöpperpieper, Phys. Rev. B (to be published).